

Investigation of the Curing Process of Spray Polyurea Elastomer by FTIR, DSC, and DMA

Qing Zhou,^{1,2} Li Cao,^{1,3} Qing Li,¹ Yalin Yao,¹ Zhaofei Ouyang,^{1,2} Zhiqiang Su,¹ Xiaonong Chen³

¹Key Laboratory of Beijing City on Preparation and Processing of Novel Polymer Materials, Beijing University of Chemical Technology, Beijing 100029, People's Republic of China

²Beijing Research Institute of Yantai Wanhua Polyurethanes Co., Ltd, Beijing 102200, People's Republic of China

³Key Laboratory of Carbon Fiber and Functional Polymers, Ministry of Education, Beijing University of Chemical Technology, Beijing 100029, People's Republic of China

Received 2 March 2011; accepted 19 December 2011

DOI 10.1002/app.36674

Published online in Wiley Online Library (wileyonlinelibrary.com).

ABSTRACT: The curing process of a typically formulated spray polyurea elastomer (SPUA) system has been thoroughly investigated with the help of a combined analysis of Fourier transform infrared spectroscopy, differential scanning calorimetry, and dynamic mechanical analysis. The evolution of the microstructure and mechanical responses of the SPUA system during the curing process have been described in detail. The experimental results indicated that the fast curing property of SPUA, which mainly based on the reaction between the primary amine groups and the isocyanate groups, led to the formation of the unstable hard segments in the interphase. After the tack-free time, the residual isocyanate groups contin-

ued to react with the rest of the secondary amine groups of the chain extenders for several hours and caused the increase of the molecular weight of the hard segment in SPUA. Furthermore, during the curing process, the "disordered" hydrogen bond formed by one C=O and one nearby NH (secondary amine) reconstructed to "ordered" bond, which contributed to the increase of the content of the hard segment and ultimately, improved the mechanical properties of the SPUA system greatly. © 2012 Wiley Periodicals, Inc. *J Appl Polym Sci* 000: 000–000, 2012

Key words: polyurea elastomer; curing process; FTIR; DSC; DMA

INTRODUCTION

Polyurethane (PU), being first discovered by Otto Bayer and his coworkers in 1937, has been explored to be a popular industrial material with comprehensive and excellent performances till now.¹ The diversified properties of PU have enabled itself to be applied as various products, including thermal plastic elastomer, coating, adhesives, sealing materials, fibers, foamed plastics, and so on.^{1–12}

Elastomeric urethane coating has become available since the 1970s and has been ever broadly used. When compared with PU, polyurea is more favorable in some special environments (such as high hu-

midity, low temperature). Furthermore, due to its fast curing ability and the combination of high flexibility with hardness, it is also a good choice when requirements such as fast curing, good abrasion, and chemical resistance are put forward.

In general, a typical PU-polyurea elastomer (PUU) has a soft phase and a hard phase in its structure, which leads to a phase separation for their thermal incompatibility. The block polymer chain comprises of three main components, a polyol, a diisocyanate, and a chain extender. The degree of the phase separation and the content of the hard segment determine the mechanical properties of the PUU system, and various formulations were found to prepare products according to their applications,^{3–9} which provides great enhancement on the mechanical properties of the polyurea material. By varying the parameters of the processing period, the targeted chain structure was achieved and the aimed application was fulfilled. Furthermore, by using diphenyl-methane-diisocyanate (MDI) as the prepolymer, the resulted spray polyurea elastomer (SPUA) become a more environmentally friendly material, because it release less volatile and toxic compounds comparing with its counterpart TDI.¹⁰ Although many research works on polyurea elastomer have been reported in the past,^{11–16} the curing mechanism of SPUA which is actually of great importance in industry has not been well explored as yet.

To better understand the mechanism of the structure formation in the curing process and further

Correspondence to: Z. Su (suzq@mail.buct.edu.cn) or X. Chen (chenxn@mail.buct.edu.cn).

Contract grant sponsor: Alexander von Humboldt Foundation.

Contract grant sponsor: National Natural Science Foundation of China (NSFC); contract grant number: 20974010.

Contract grant sponsor: Beijing New-Star Program of Science and Technology; contract grant number: 2009B10.

Contract grant sponsor: Fundamental Research Funds for the Central Universities; contract grant number: ZZ1007.

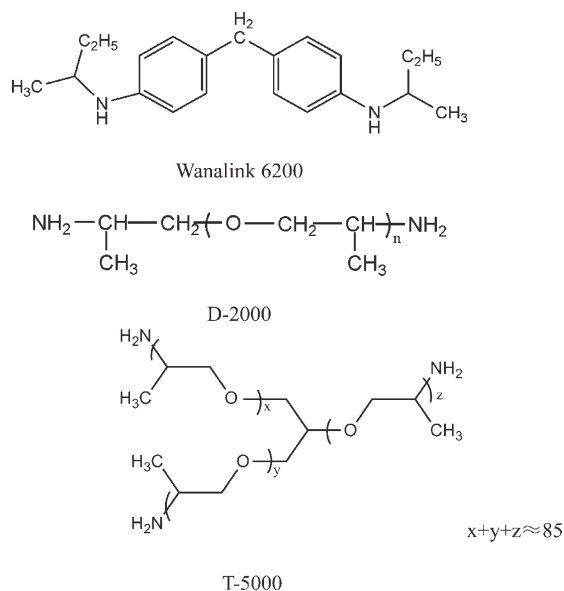
Contract grant sponsor: Program for Changjiang Scholars and Innovative Research Team in University (PCSIRT); contract grant number: IRT0807.

adjust the technology conditions to acquire better properties, the structural change of soft and hard segments of SPUA in every curing moment was observed by Fourier transform infrared spectroscopy (FTIR), differential scanning calorimetry (DSC), and dynamic mechanical analysis (DMA). In addition, the influence of the structural change on the mechanical properties of the material was also investigated. The study is helpful for us to understand the structural evolution of SPUA in the curing process and to produce high performance SPUA materials in the future.

EXPERIMENTAL

Materials

Commercial MDI prepolymers, WANNATE 8312, NCO = 15.5%, with a viscosity of 700 mPa·s at 25°C, were purchased from Yantai Wanhua Polyurethanes, and WANNATE 8312 is a modified diphenylmethane diisocyanate (MDI), containing relatively high level of 2,4'-MDI. It is a light yellow liquid at room temperature, specially designed for polyurea spray elastomer applications, polyether amines JEFFAMINE® D-2000 and JEFFAMINE® T-5000 from Huntsman are amines linked by poly (propylene oxide) (PPO), and the designation number refers to the approximate molecular weight of each species, D and T means difunctional and trifunctional, respectively. Chain extenders DETDA (diethyl-toluenediamine) and WANALINK 6200 were also purchased from Yantai Wanhua Polyurethanes. All of these materials were used without any further treatment or purification.



Preparation of SPUA samples

Wannate 8312 as **A** component, a formulated mixture of D-2000, T-5000, DETDA, Wanlink 6200 with

a content of 60.0, 7.5, 18.0, and 14.5%, respectively, as **B** component were used in the preparation of the samples with a ratio of NCO/(NH+NH₂) 1.079.

SPUA samples were prepared by using a GUSMER® H-20/35 spray machine equipped with a GUSMER® GX-7 Series 400 spray gun. In all spray runs, block and hose heaters were set at 70°C with a system pressure of 140 MPa. Film samples of 2-mm-thick were obtained by the application of the polyurea spray coatings onto 12 cm × 12 cm polypropylene board without any release agent. The volume mixing ratio of **A** and **B** components is 1 : 1.

Sample characterizations

The test samples were collected at different times of the curing process, and the test methods included FTIR, DSC, and DMA.

FTIR measurements

IR spectra of all samples were measured at 26°C using a Nicolet Magna 750 FTIR spectrometer equipped with a DTGS detector. The spectra were collected at a resolution of 4 cm⁻¹ with 16 scans. The measured wave number range was 400–4000 cm⁻¹. All the original spectra were baseline corrected using OMNIC 5.1 software before curve fitting.

DSC measurements

The calorimetric measurements were performed with a Mettler DSC 822e differential scanning calorimeter at a heating rate of 10°C/min in a flowing N₂ atmosphere, and the sample weight was about 10 mg. Indium was used as the standard sample.

DMA measurements

The dynamic mechanical properties were measured on a DMA Q800 (TA instruments) at a frequency of 1Hz. The heating rate was 3°C/min, with amplitude at 20 μm. Rectangular bars of 2.0 mm × 5.3 mm × 20 mm were cut for tensile testing.

RESULTS AND DISCUSSIONS

Segmented poly(urethane urea) elastomers exhibit versatile physical properties, and microphase separation of multiblock PU copolymers into “soft” and “hard” domains is believed to be responsible for the versatile properties of this category of materials.¹⁷ A large number of previous investigations have been reported on the characterization of microdomain structure.^{18–21}

In this work, a typical SPUA formulation as described before was investigated by tracing its curing process with FTIR, DSC, and DMA, and the corresponding mechanical properties were also studied to depict the morphology evolution during the curing process. In order to specifically understand the role of each component of the elastomer, several model compounds were synthesized and measured as following:

W8312 soft segment has a glass transition at -58°C , W8312 with DETDA (1 : 1 mol ratio) hard segment at 237°C , W8312 with D2000 (1 : 1 mol ratio) hard segment at 238°C , W8312 with T5000 (1 : 1 mol ratio) hard segment at 278°C , and W8312 with Wanalink 6200 (1:1 mol ratio) hard segment at 178°C .

FTIR analysis

FTIR, DSC, and DMA have always been the reliable and mature means to study PU structure.^{18–26} For FTIR analysis,^{18–23} there is a consensus that the absorbance at $1632\sim 1643\text{ cm}^{-1}$ indicates the hydrogen bonding formed by one C=O with two nearby N–H in urea group, which is conventionally called “ordered” bonding. C=O may also form hydrogen bond with only one N–H nearby, which is accordingly called “disordered” bonding, with a absorbance region of $1678\sim 1659\text{ cm}^{-1}$. Additionally, the absorbance at 1728 cm^{-1} represents the C=O bond in urethane, and 2263 cm^{-1} for the N=C=O absorbance. In this work, a series of samples were obtained at different times during the curing process to undergo FTIR analysis.

FTIR spectra of SPUA samples at different curing times are shown in Figure 1. It indicates a regular change of C=O absorbance intensity at 2263 , 1728 , 1673 , and 1643 cm^{-1} , respectively, in the curing process. In order to characterize the change of IR band intensities in quantities, the absorbance intensities of different IR bands were measured and normalized with the benzene absorbance at 1600 cm^{-1} . The results are shown in Figure 2.

Figure 2(a) shows a logarithmic relationship of the NCO absorbance (2263 cm^{-1}) with the curing time after spraying. NCO absorbance intensity decreases rapidly in the first 430 min and keeps decreasing until equilibrium is reached at 1440 min, which indicates that a large part of NCO has reacted with the primary amine as quickly as spraying is performed, and the residual NCO groups has kept reacting to the secondary amine groups. Therefore, the viscosity of the system become extremely high, but for the relatively slow reaction rate of the secondary amine, the consumption of NCO in the curing process slows down, and reaches an end about 24 h later.

In Figure 2(b), absorbance at 1643 cm^{-1} is the vibration of polyurea C=O formed by the primary

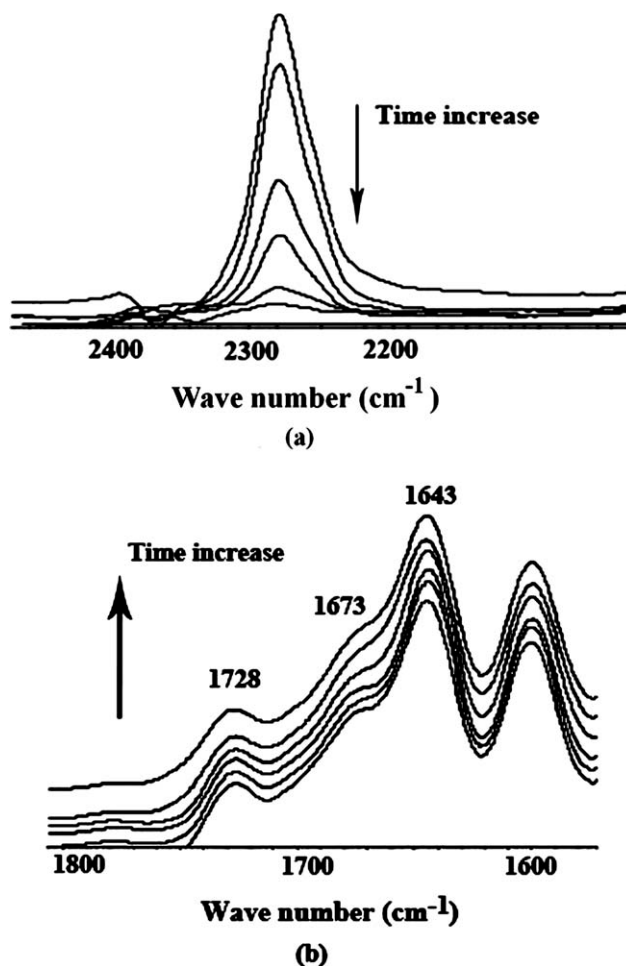


Figure 1 FTIR spectra of SPUA sample at different curing times (a) IR absorbance peak at 2263 cm^{-1} (b) IR absorbance peaks at 1728 , 1673 , and 1643 cm^{-1} , respectively.

amine of D2000, T5000, and DETDA, with NCO groups in prepolymer. C=O also formed “ordered” hydrogen bonding with two nearby N–H, which forms the hard phase. The absorbance at 1643 cm^{-1} ascends rapidly and quickly reaches equilibrium afterward. This indicates that the formation of the hard phase is almost completely completed during the first 400 min.

In Figure 2(c), the absorbance at 1673 cm^{-1} indicates the vibration of urea C=O originated from the reaction of secondary amine (Wanlink6200) to NCO in the prepolymer. The “disordered” hydrogen structure of C=O with N–H nearby results in an interphase of soft and hard segments. The absorbance intensity increases slowly after a sharp upward trend in the first 430 min due to its weak reactivity compared to primary amine. Although the reaction of primary amine to NCO produces a fast increase in the first 430 min, the slow reaction of secondary amine has made the control of the reaction rate of the whole system available, which provides a facility to spray operation.

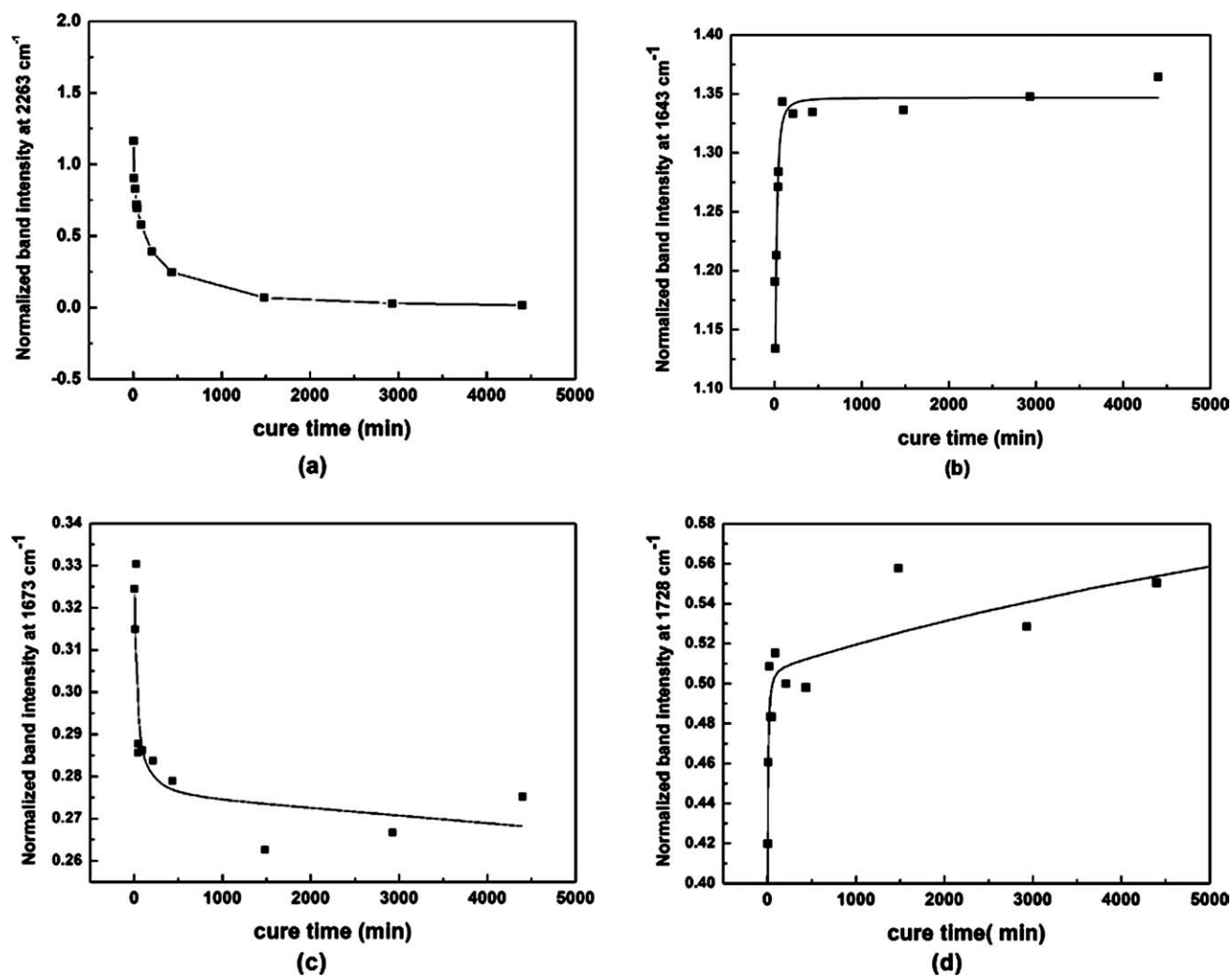


Figure 2 The change of IR bands intensities at different curing times. (a) 2263 cm^{-1} band; (b) 1643 cm^{-1} band; (c) 1673 cm^{-1} band; (d) 1728 cm^{-1} band.

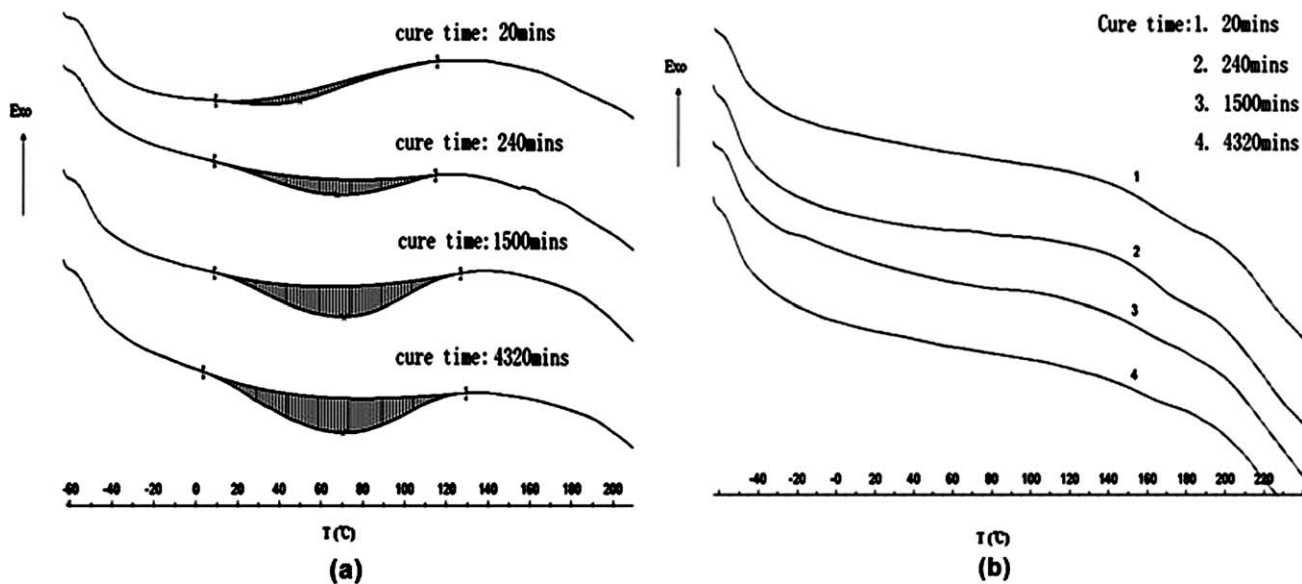


Figure 3 (a) DSC heating thermograms of SPUA samples with different curing times; (b) DSC heating thermograms of annealed SPUA samples with different curing times, annealing temperature is 130 $^{\circ}\text{C}$.

TABLE I
DSC Data of SPUA Samples at Different Curing Times

Cure-time(min)	T_{gs} -first scan		T_{gs} -annealing at 130°C		Endotherm of the hard segment relaxation-first scan	
	ΔC_{ps1st}^a ($J g^{-1} K^{-1}$)	Midpoint ($^{\circ}C$)	ΔC_{ps2nd}^b ($J g^{-1} K^{-1}$)	Midpoint ($^{\circ}C$)	ΔH^c ($J g^{-1}$)	Temperature ($^{\circ}C$)
20	0.281	-48	0.212	-46	-1.94	13.14 ~ 88.62
240	0.231	-50	0.224	-46	-4.29	18.04 ~ 111.53
1500	0.213	-51	0.229	-48	-7.65	16.99 ~ 116.37
4320	0.209	-51	0.213	-48	-9.44	17.43 ~ 116.79

^a ΔC_{ps1st} is the change of heat capacity of soft segment in first scan.

^b ΔC_{ps2nd} is the change of heat capacity of soft segment after annealed at 130°C for 5 min.

^c ΔH is endotherm of the hard segment relaxation.

In Figure 2(d), absorbance at 1728 cm^{-1} is the C=O vibration of urethane groups in prepolymer W8312. As the curing proceeds, it shifts to a lower wave number of 1700 cm^{-1} , and because of the hydrogen bonding formed by urethane C=O with urea groups, the peak intensity at 1728 cm^{-1} decreased. FTIR results confirm that after reacting for a long time the monomer of chain extender Wanalink6200 still exists.

DSC analysis

SPUA is a typical multiblock copolymer, including several patterns of morphology comprised of hard segments and soft segments. In the curing process, the microphase separation is more complex, for there are residual reactions as shown above. DSC is the most attractive tool for phase separation study^{9,10,15,17,19} and the thermal properties measured by DSC are reported in Figure 3 and Table I. All materials are phase-segregated, with a low glass transition temperature of the soft phase.

The curing process takes place at $70^{\circ}C$, higher than the glass transition point of soft segment, and far below the glass transition point of hard segment,

which is about $178^{\circ}C$ at least, so the curing reaction, as well as chain extending process, is thermal dynamically inclined to happen in the soft segments region. Thus, an interphase mixture of hard segments and soft segments is formed in the SPUA system.

Table I and Figure 3(a) show that the ΔC_{ps1st} (the change of heat capacity of soft segment in first scan) decreases as the curing time elongates. In the curing process, the low molecular oligomer, which is reasonably assumed to be oligomer from the Wanalink 6200, reacts into the molecular chain as the hard segment, and forms an interphase by mixing with the soft segment in which the hard segment is not thermodynamically miscible with the soft segment. Besides, the curing reaction happens at a temperature which is far below the T_g of hard segments, thus the new generated hard segments become frozen in the interphase and possess thermodynamic potential for the molecules to approach equilibrium state by undergoing further packing and conformation changes. Meanwhile, the soft segment's motion suffers entropy restriction effect from the interphase connection, which would lower the ΔC_{ps1st} value, as Table I shows. As the molecular weight increases, the interphase enlarges as a result of more hard segments freezing into it, which will give rise to more

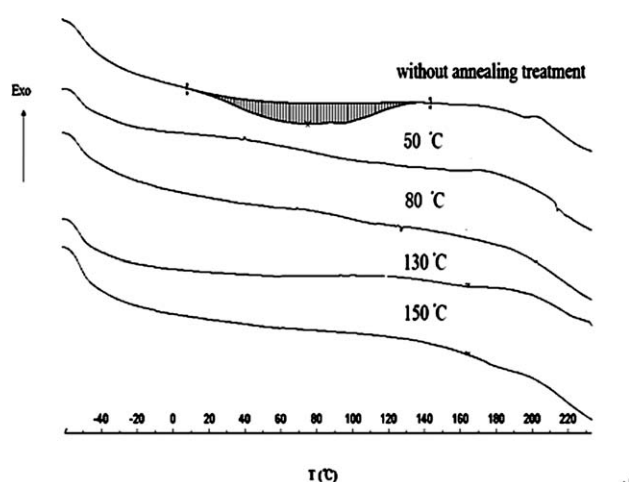


Figure 4 DSC heating thermograms of annealed SPUA samples with different annealing temperatures.

TABLE II
DSC Data of Different Annealed SPUA Samples

Annealing temperature ($^{\circ}C$)	T_{gs}		T_{gh}	
	ΔC_{ps}^a ($J g^{-1} K^{-1}$)	Midpoint ($^{\circ}C$)	ΔC_{ph}^b ($J g^{-1} K^{-1}$)	Midpoint ($^{\circ}C$)
No	0.176	-52	-	-
50	0.178	-54	-	-
80	0.198	-53	-	-
130	0.200	-53	0.062	145
150	0.226	-52	0.159	162

^a ΔC_{ps} indicates the change of heat capacity of soft segment.

^b ΔC_{ph} indicates the change of heat capacity of hard segment.

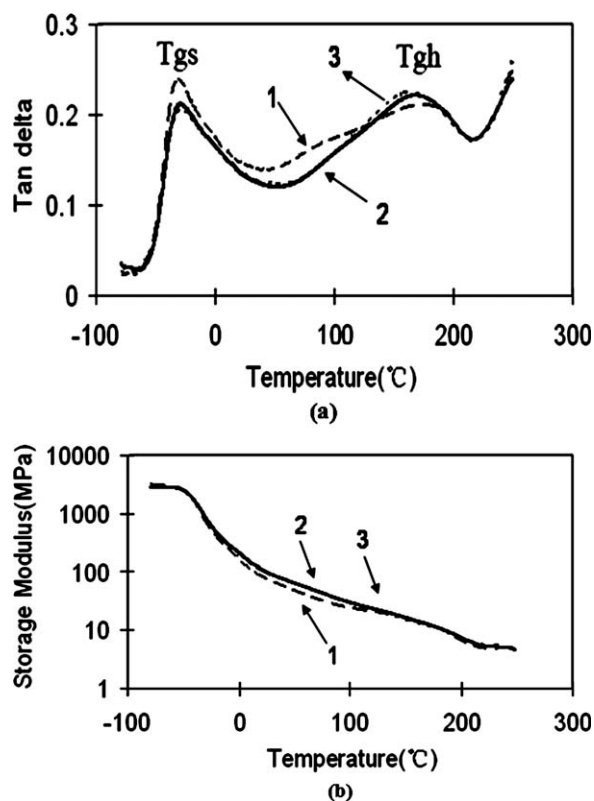


Figure 5 DMA diagram of SPUA sample at different curing times; curve 1: curing time is 220 min; curve 2: curing time is 1520 min; curve 3: curing time is 8d; (a) $\tan \delta$; (b) storage modulus.

restriction to soft segments and decrease the ΔC_{ps1st} value.

It is known that the chain extender, Wanlink 6200, reacts into the molecular chain gradually and most possibly exists in the interphase as the hard segments. At low temperature and high viscosity, the hard segments in interphase are frozen in an unstable state with an intense inner stress, which could be released through annealing treatment. As is shown in Figure 3(b) that after being annealed at 130°C for 5 min the endotherm in the first scan is vanished, which can be explained that the free volume of the molecular chain expands when the sample is annealed, and the frozen chain gets relaxed. In Table I, the endotherm of the hard segment (ΔH) increases with the curing time obviously, with a reason that while the chain extender reacts into the interphase as hard segment part, the molecular weight of the hard phase increases as well.

As is shown by Figure 4, the endotherm peak of ΔH disappears when the sample is annealed. This indicates that the endotherm peak from 10 to 120°C is a typical molecular chain relaxation movement. The wide range of the peak is ascribed to the movements of various lengths of hard segments in the interphase. In Table II, DSC thermograms data of

the samples annealed at different temperatures is reported. It shows that the ΔC_{ps} increases as the annealing temperature rising from 50 to 150°C, which can be explained that when the annealing temperature gets close to the hard segment's T_g , the free volume expands enough for the frozen hard segment to move. Under the drive of the thermodynamic potential in the unstable interphase, the hard segments tend to separate from the soft segment phase as soon as it can move. In the meantime, as the phase separation proceeds, the content of the hard segment phase increases, and the ΔC_{ps} doubled when the temperature gets close to the T_g of the hard segment of 178°C, which refers to the T_g of the model, W8312 with Wanalink 6200.

Dynamic mechanical analysis

Figure 5 shows the DMA data of SPUA samples at different curing times. In Figure 5(a), the DMA spectra have two $\tan \delta$ peaks, T_{gs} at -40°C and T_{gh} at 170°C . T_{gs} and T_{gh} refer to soft segment glass transition and hard segment glass transition, respectively,^{19,22,27} and the T_{gh} peak is apparently wider. Based on the discussion of DSC results in the former section, it is easy to deduce that, as temperature rises, the frozen hard segments in interphase relax gradually, which make the T_{gh} peak wide. In curve

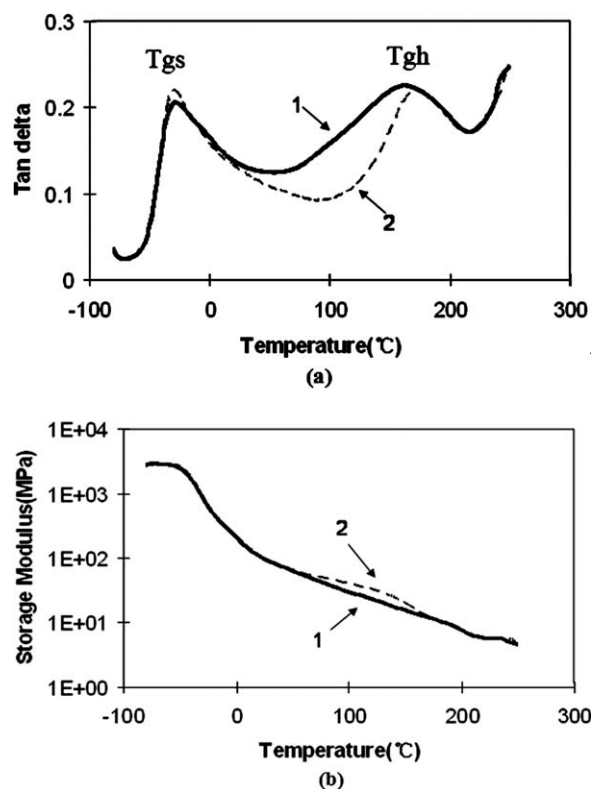


Figure 6 DMA diagram of SPUA samples; curve 1: SPUA sample without annealing treatment; curve 2: SPUA sample annealed at 130°C for 1 h; (a) $\tan \delta$; (b) storage modulus.

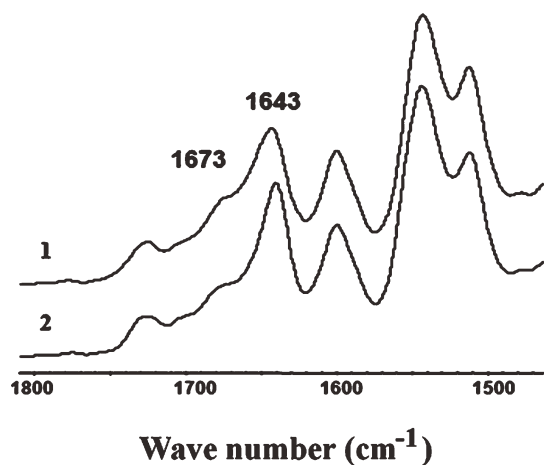


Figure 7 FTIR spectra of SPUA samples; curve 1: SPUA sample without annealing treatment; curve 2: SPUA sample annealed at 130°C for 1 h.

1, there is obviously a shoulder at 80°C between the T_{gs} and T_{gh} , which decreases to a constant value as curve 2 and curve 3 with the curing time elongating, as the hard segment part increases to a final equilibrium state, the storage modulus apparently increases [Fig. 5(b)].

Figure 6 shows a DMA spectrum of the sample annealed at 130°C for 1 h. After annealing, the storage modulus of the rubbery plateau from 0 to 130°C is obviously higher and more flat. The tan delta peak at T_{gs} is higher after annealed, and the two peaks, T_{gh} and $T_{gs'}$ split apart apparently and become sharper. All these indicate that phase separation has occurred. Under annealing treatment, the hard segments in interphase are enabled to move and reconstruct. In Figure 7, the FTIR spectra show that after being annealed, the absorbance band at 1673 cm^{-1} , regarding to the urea carbonyl of the interphase, moves to lower wave number of 1643 cm^{-1} , and the peak is narrower and higher, demonstrating that the disordered urea hydrogen bond, existing in the interphase, has reconstructed into an ordered hydrogen bond, which is more thermostable and stronger in mechanical properties. The result is in good consistence with the DSC and DMA conclusions.

CONCLUSIONS

The reaction between the primary amine and the NCO group in MDI gives rise to the fast curing property of SPUA system, whereas the secondary amine with a slow reactivity provided the facility to spray operation by controlling the reaction rate, and increased the molecular weight of the hard segment out of the tack free time, which is the main reason to produce improvement in the mechanical property of SPUA.

Through collecting samples at intervals, we depicted the structural evolvement timely in the curing process. During the curing process, the content of hard segments in interphase increases by its best, and because the curing temperature is far below the T_{gh} , the hard segment chain in the interphase is in an unstable state with an intense inner stress, which contributes to a thermodynamic potential for the molecules to approach equilibrium state through further packing and conformation changes. As the frozen hard segment reconstructed, the disordered hydrogen bond reconstructed to ordered bond, which comprise the hard phase. Meanwhile, more restrictions are formed to stop the movement of the soft segment, which lower the ΔC_{ps1st} . At the end, the increase of the content of hard phase leads to clear phase separation and the improvement of the mechanical properties of SPUA.

References

- Hepburn, C. *Polyurethane Elastomers*; Elsevier, Applied Science: Amsterdam, 1992.
- Garrett, J. T.; Runt, J.; Lin, J. S. *Macromolecules* 2000, 33, 6353.
- Cella, R. J. *J Polym Polym Symp* 1973, 42, 727.
- Lilaonitkul, A.; West, J. C.; Cooper, S. L. *J Macromol Sci Phys* 1976, 12, 563.
- Lilaonitkul, A.; Cooper, S. L. *Rubber Chem Technol* 1977, 50, 1.
- Bonart, R. *J Macromol Sci Phys B* 1968, 2, 115.
- Bonart, R.; Morbitzer, L.; Hentze, G. *J Macromol Sci Phys* 1969, B3, 337.
- Koberstein, J. T.; Gancarz, I.; Clarke, T. C. *J Polym Sci Polym Phys* 1986, 24, 2487.
- Lee, H. S.; Hsu, S. L. *Macromolecules* 1989, 22, 1100.
- Yeh, F. J.; Hsiao, B. S.; Sauer, B. B.; Michel, S.; Siesler, H. W. *Macromolecules* 2003, 36, 1940.
- Elwell, M. J.; Ryan, A. J.; Grunbauer, H. J. M.; Van Lieshout, H. C. *Polymer* 1996, 37, 1353.
- Mcclusky, J. V.; Priester, R. D.; O'Neill, R. E.; Willkomm, W. R.; Heaney, M. D.; Capel, M. A. *J Cell Plast* 1994, 30, 338.
- Priester, R. D.; Mccluskey, J. V.; O'Neill, R. E.; Turner, R. B.; Harthcock, M. A.; Davis, B. L. *J Cell Plast* 1990, 26, 346.
- Li, W.; Ryan, A. J.; Meier, I. K. *Macromolecules* 2002, 35, 6306.
- Chen, T. K.; Shieh, T. S.; Chui, J. Y. *Macromolecules* 1998, 31, 1312.
- Garrett, J. T.; Siedlecki, C. A.; Runt, J. *Macromolecules* 2001, 34, 7066.
- Chen, T. K.; Chui, J. Y.; Shieh, T. S. *Macromolecules* 1997, 30, 5068.
- Teo, L. S.; Chen, C. Y.; Kuo, J. F. *Macromolecules* 1997, 30, 1793.
- Garrett, J. T.; Xu, R. J.; Cho, J. D.; Runt, J. *Polymer* 2003, 44, 2711.
- Coleman, M. M.; Skrovanek, D. J.; Hu, J. B.; Painter, P. C. *Macromolecules* 1988, 21, 59.
- Luo, N.; Wang, D. N.; Ying, S. K. *Polymer* 1996, 37, 3577.
- Jena, K. K.; Raju, K. V. S. N. *Ind Eng Chem Res* 2008, 47, 9214.
- Garrett, J. T.; Lin, J. S.; Runt, J. *Macromolecules* 2002, 35, 161.
- Choi, T.; Weksler, J.; Padsalgikar, A.; Runt, J. *Polymer* 2009, 50, 2320.
- Yilgor, I.; Yilgor, E.; Guler, I. G.; Ward, T. C.; Wilkes, G. L. *Polymer* 2006, 47, 4105.
- Fragiadakis, D.; Gamache, R.; Bogoslovov, R. B.; Roland, C. M. *Polymer* 2010, 51, 178.
- Samson, N.; Mechin, F.; Pascault, J. P. *J Appl Polym Sci* 1998, 70, 2331.